DOI 10.1002/eji.201040588 Eur. J. Immunol. 2010. 40: 1836–1842

Review Series 14th ICI

Basophils are potent antigen-presenting cells that selectively induce Th2 cells

Kenji Nakanishi[1,2]

[1] Department of Immunology and Medical Zoology, Hyogo College of Medicine, Nishinomiya, Hyogo, Japan
[2] Collaborative Development of Innovatioin Seeds, Japan Science and Technology Corporation, Saitama, Japan

Basophils and mast cells are important effector cells in helminth-infected host and IgE-mediated allergic inflammation. Although they have the same progenitors, basophils and mast cells complete their terminal differentiation in the bone marrow and peripheral tissues, respectively, and only basophils circulate in the blood. Although it is recognized that basophils are important for Th2 responses, and it is also well established that IL-4 is required for Th2 differentiation from naïve CD4$^+$ T cells, the nature of the cells that produce "early" IL-4, remained elusive until recently. Three groups independently demonstrated that basophils are the predominant APC in inducing Th2 response against helminth parasites and allergens. Basophils express MHC class II and CD80/86, have the potential to take-up and process protein Ag (particularly Ag–IgE complex) and to present peptide in the context of MHC class II, and to produce IL-4. These Ag-pulsed basophils induce the development of Th2 cells both *in vitro* and *in vivo*. Thus, basophils contribute to Th2/IgE response by the production of IL-4 and presentation of MHC class II/peptide complex to naïve CD4$^+$ T cells, in contrast to the Th1-inducing action of DC. In this review, we summarize what is known regarding basophil function in allergy and parasite infection, examine the novel Ag-presenting function of basophils and discuss potential clinical implications of this finding.

Key words: Ag–IgE complex · Basophils · Helminth infection · Th2 response

Introduction

Mast cells, basophils and eosinophils are key effector cells in response to parasite infection and allergic inflammation [1–5]. Basophils and eosinophils are granulocytes, which mature in the bone marrow, circulate in the blood and are recruited to allergic inflammatory sites [3–5]. In contrast, progenitors of mast cells migrate from the bone marrow to the peripheral tissues and undergo their terminal differentiation *in situ*; mast cells that complete their differentiation in the skin or intestine develop into connective tissue mast cells and mucosal mast cells, respectively [1, 2]. Mast cells and basophils express the high-affinity receptor for IgE and, upon crosslinking of FcεR1-bound IgE with multivalent Ag, rapidly produce diverse preformed mediators, cytokines (*e.g.* IL-4 and IL-13) and lipid mediators, leading to the induction of immediate-type hypersensitivity [1–5]. Here, the author reviews the major functions of basophils as effector cells in the development of allergic inflammation and their novel function as Th2-inducing APC in helminth infection and allergy.

Correspondence: Prof. Kenji Nakanishi
e-mail: nakaken@hyo-med.ac.jp

Basophil development and its role in allergy

As mentioned, mast cells, basophils and eosinophils are the key innate effector cells involved in parasite-induced immune responses and allergic inflammation. Basophils are short-lived cells that account for less than 1% of circulating granulocytes in the blood. In contrast, mast cells are located in the tissue and mast cell progenitors have the potential to proliferate locally in the tissue in response to IL-3, IL-4 and IL-9, resulting in local mastocytosis.

A study by Arinobu *et al.* [6] has identified a common progenitor of basophils and mast cell precursor (BMCP), which arise from the granulocyte/monocyte progenitor (GMP). Eosinophil precursor also arises from GMP. The development from GMP to eosinophil precursor and BMCP, and from BMCP to basophil precursor or MCP, are regulated by the level and order of expression of transcription factors, C/EBPα and GATA-2 [6]. Morphologically, basophils and eosinophils have lobulated nucleus and secretory granules in the cytoplasm. Mast cells are round cells with a non-segmented nucleus and intracellular granules. Although basophils and mast cells are heterogeneous in their development and morphology, they are regarded to share a pathological role in allergic responses, as demonstrated by their potential to produce cytokines, vasoactive histamine and lipid mediators after FcεR1 crosslinkage [1–5]. Thus, individuals with atopy, after repeated exposure to a particular Ag such as pollen, exhibit immediate-type hypersensitivity. Furthermore, there is tight correlation between FcεR1 expression on basophils and IgE level in human peripheral blood [7], suggesting a positive feedback mechanism for the IgE-mediated immediate-type hypersensitivity reaction [8, 9]. Thus, once individuals with atopy start to produce IgE, they develop progressive allergic inflammation by increasing production of IgE and expression of FcεR1 on effector cells.

Basophil activation in parasitic infection and allergic inflammation: Role of IL-3

There appears to be at least two major pathways of basophil activation during allergic inflammation, one involving Ag/IgE signaling and the other that is mediated by PAMP and soluble mediators such as IL-18 and IL-33.

An important cytokine involved in both pathways of basophil activation is IL-3. IL-3 is not only an important growth factor for mast cells and basophils, IL-3 stimulation also induces basophil production of IL-4. Furthermore, basophils, when stimulated with a combination of IL-3 and crosslinking of FcεR1 by Ag, strongly produce IL-4 and IL-13, suggesting the importance of crosstalk between IL-3-mediated signaling and FcεR1-mediated signaling for IL-4 and IL-13 production. Furthermore, FcR common γ-chain (FcγR) may also be important in basophil activation. Recently, Hida *et al.* [10] demonstrated that basophils lacking FcγR could proliferate normally but failed to produce IL-4 in response to IL-3, suggesting that FcγR-mediated IL-3 signal is crucial in IL-4 production by basophils.

The effect of IL-3 can also be observed in IgE-independent basophil IL-4 production. We previously demonstrated that basophils express IL-18R and IL-33R and produce IL-4, IL-6, IL-13 and chemical mediators when stimulated with IL-3 plus IL-18/IL-33 *in vitro* (Fig. 1, left panel) [11, 12]. These results suggest the potential of basophils to induce allergic inflammation in an IgE-independent manner (innate-type allergic inflammation). Mouse basophils also express TLR1, TLR2, TLR4 and TLR6 and produce Th2 cytokines including IL-4 and IL-13 in response to stimulation with TLR ligands plus IL-3 [13].

Thus, as stated, there are at least two major basophils activation pathways during allergic inflammation. One is an Ag/IgE-dependent pathway responsible for "acquired-type allergic inflammation" and the other is an IL-18, IL-33 or PAMP-dependent pathway responsible for "innate-type allergic inflammation."

IL-3 is also important for generation and peripheral accumulation of basophils during parasitic infections [14]. Infection of wild-type mice with *Strongyloides venezuelensis* or *Nippostrongylus brasiliensis* causes accumulation of basophils in the liver and spleen of the host [15]; however, this accumulation is not observed in IL-3-deficient mice [14]. Thus, IL-3 produced by Th2 cells is critically involved in generation, accumulation and activation of basophils.

In terms of the interactions between allergic inflammation and parasitic infection, we showed previously that nasal administration of IL-18 or IL-33 induces bronchial asthma entirely independently of allergen and IgE [12, 16]. As these cytokines are stored in the epithelial cells, infection with pathogens, including helminth parasites, bacteria, fungi and viruses or exposure to allergens, can induce the release of IL-18 and IL-33 from epithelial cells, causing IL-18 and/or IL-33-mediated allergic inflammation (Fig. 2), which is dependent on IL-18R and/or IL-33R and the adapter protein MyD88 pathway (Fig. 1). Basophils and mast cells also produce Th2 cytokines in response to parasite Ag (*e.g.* IPSE-α-1, a soluble glycoprotein Ag from eggs of *Schistosoma mansoni* and has been shown to stimulate basophils in an IgE-specific but Ag-nonspecific manner [17]). Basophils and mast cells may also respond to other parasite Ag, suggesting their role in defense against intestinal nematode such as *S. venezuelensis*, *N. brasiliensis* or *Trichuris muris*. Eosinophils are also effector cells of parasite infection – they defend against the tissue stage of helminth that is too large to be phagocytosed. IgE antibodies that bind to the surface of helminths activate eosinophils to produce granule content such as the major basic protein, which is highly toxic to helminths. Recruitment of eosinophils is also a well-known late hallmark of allergic inflammation and contributes to pathological processes in allergic diseases. Thus, basophils, mast cells and eosinophils are major effector granulocytes in parasitic infection and allergic inflammation.

Basophils in chronic allergic inflammation and systemic anaphylactic shock

Recent studies suggest that basophils also induce IgE-mediated chronic allergic inflammation and IgG1-mediated systemic anaphylactic shock [4, 18, 19]. Mukai *et al.* demonstrated that a single injection of multivalent Ag in the ear of mice passively sensitized with Ag-specific IgE induces immediate-phase, late-phase and delayed-onset of ear swelling characterized by infiltration with basophils and eosinophils [18]. Mast cell-deficient mice did not develop immediate- and late-phase ear swelling, suggesting mast cells are responsible for inducing these ear swellings. In contrast, depletion of basophils in wild-type mice diminished delayed-onset of ear swelling and eosinophilic infiltration. Moreover, transfer of basophils into FcεR1-deficient mouse showed that basophils are responsible for inducing delayed-onset ear swelling that is

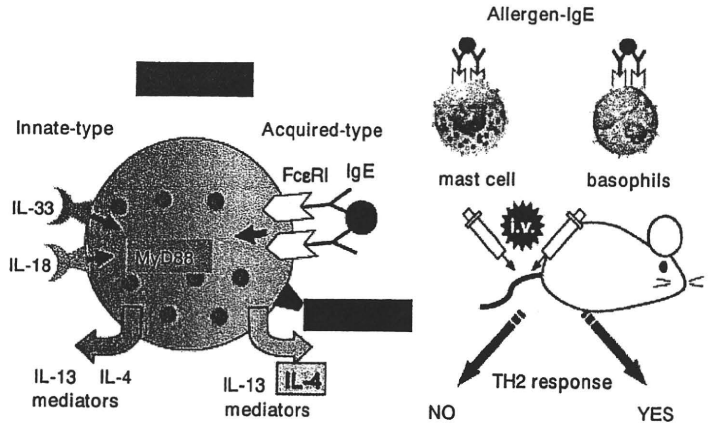

Basophils are APC that can specifically induce Th2 cells.

Figure 1. Basophils are effectors cells and also inducers of Th2 response *in vivo*. Basophils, which produce IL-4, IL-13, and other mediators when stimulated with IL-3 plus Ag/IgE complex (acquired-type activation) also produce these cytokines and mediators, when stimulated with IL-3 plus IL-18 or IL-3 plus IL-33 (innate-type allergy). Furthermore, intravenous administration of basophils (but not mast cells) pulsed with allergen induce the development of Th2 cells in the peripheral lymphoid organs.

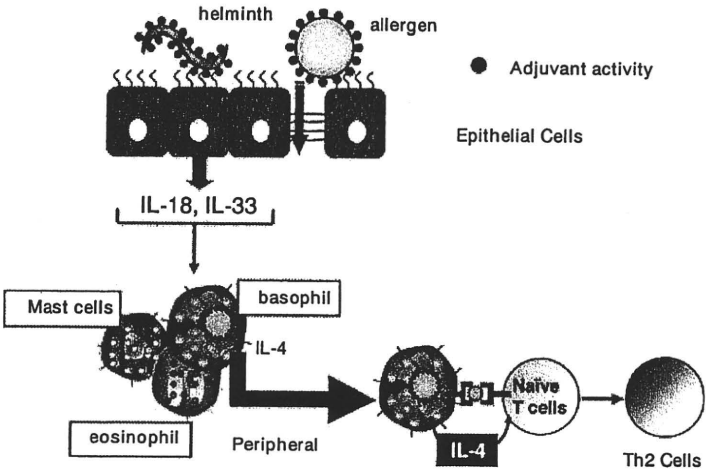

Figure 2. Interaction between epithelial cells and basophils. IL-18 or IL-33 derived from epithelial cells stimulated with helminth or allergen induces mast cells, basophils and eosinophils to produce Th2 cytokines, chemokines and chemical mediators. Among these granulocytes, basophils strongly produce IL-4 in response to IL-18 or IL-33. Basophils also uptake and process allergen and express allergen-derived peptide with MHC class II. These basophils prime Th2 responses in an MHC class II-dependent and IL-4-dependent manner.

associated with marked eosinophilic infiltration. Therefore, basophils seem to induce delayed-onset or chronic allergic inflammation by recruiting eosinophils [18].

It is well documented that mast cells and IgE are crucially involved in the development of systemic anaphylaxis. Interestingly, mice deficient for mast cells or IgE nevertheless develop systemic anaphylaxis, suggesting that an alternative pathway may be involved. Tsujimura *et al.* [19] clearly demonstrated that basophils and IgG1 induce mast cell-independent systemic anaphylaxis.

Role of Th cells in allergy and infection

Allergen-activated Th2 cells produce cytokines that induce allergen-specific IgE production by B cells and recruitment of mast cells, eosinophils and basophils to the site of allergic inflammation. Helminth infection also induces Th2 responses, resulting in high levels of IgE and recruitment of mast cells, eosinophils and basophils to the infected organ. Naïve $CD4^+$ T cells develop into Th1, Th2, Th17 cells and Treg upon activation by appropriate combination of antigenic signal, costimulation and cytokine signals by APC and accessory cells [20]. IFN-γ and IL-12 induce the development of Th1 cells, which are characterized by a high-level production of IFN-γ and are indispensable for eradication of intracellular pathogens [21]. IL-4 triggers the differentiation of Th2 cells [22]. Th2 cells are critically involved in clearing extracellular multi-cellular parasites such as helminths and in helping B cells to produce antibodies. Th2 cells are also involved in the pathogenesis of allergic inflammation. Th17 cells play an important role for the defense against extracellular pathogens and fungi [23]. Differentiation of Th17 cells is induced by TGF-β and IL-6 in the mouse and by TGF-β and IL-6 or IL-21 in the human [23] (see also review on IL-6 in this issue [24]). Treg can be induced by TGF-β and are involved in maintaining immune tolerance [25].

The initial source of the differentiation factors for both Th1 and Th2 cells are cells of the innate immune system responding to microbial Ag, parasitic Ag, or allergens. DC recognize bacteria through TLR and mature to express costimulatory molecules CD80/86 and to produce IL-12 and IL-18, favoring development of Th1 cells [26–28]. Thus, DC infected with intracellular bacteria induce Th1 cells.

Of particular importance to allergic inflammation and parasite infections is the nature of APC involved in polarizing Th2 responses. Ag-pulsed DC can also induce the development of Ag-specific naïve $CD4^+$ T cells into Th2 cells under the presence of IL-4 *in vitro* [20]; however, the APC involved in the development of Th2 response under physiological conditions remains uncertain. Several reports indicate that there are several pathways for the differentiation of naïve $CD4^+$ T cells into Th2 cells [29–33]. The Notch-ligand Jagged 1 and Jagged 2 on DC can trigger Th2 differentiation independently of IL-4 and STAT6 signaling [29]. Epithelial cells-derived cytokine, thymic stromal lymphopoetin (TSLP), activates DC to express OX40L, which induces the development of Th2 cells [30]. Aluminum adjuvant also induces Th2-cell differentiation, although exact mechanism remains uncertain [31]. In addition, M2 macrophages (also known as alternatively activated macrophages), eosinophils and mast cells are also important for the development of Th2 cells [32, 33].

Previous studies suggested that basophils may be critical in Th2 immunity. Min and colleagues [34] showed that naïve $CD4^+$ T cells stimulated with peptide-pulsed DC develop into Th2 cells when cultured with basophils from wild-type mice but not from IL-4-deficient mice. As both DC and basophils are added to the same culture, it was initially considered that DC deliver antigenic-specific signal and basophils promote the development of Th2 response by providing early IL-4 signal to Ag-activated $CD4^+$ T cells. It was also previously reported that helminth infection induces the development of Th2 cells and accumulation of basophils in the spleens and livers of host mice [15], suggesting that the relationship between Th2 cells and basophils may be more direct. *In vivo*, mice deficient in interferon-regulatory factor 2 show expansion of basophil and spontaneous Th2 differentiation [35], suggesting promotion of Th2 immune response by basophils. Furthermore, this Th2 differentiation is markedly reduced by the introduction of mutation in the gene-encoding c-Kit, because this mutation reduces the number of basophils [35]. Thus, although indirect evidence support the role of basophils in Th2 immunity, it is important to formally prove that basophils produce "early" IL-4, required for the development of naïve $CD4^+$ T cells into Th2 cells. Recently, three groups independently demonstrated that basophils and not DC, are the critical APC involved in Th2 differentiation *in vivo* [36–38].

Th2 development: Basophils as IL-4 provider

Medzhitov and colleagues [39] previously reported that basophils are important for the development of Th2 cells in response to papain. At day 3 after papain stimulation, basophils migrated into the T-cell zones of the draining lymph nodes, in which the basophils produce IL-4 and/or TSLP, which promote Th2 differentiation *in vivo*. Papain is a cysteine protease hydrolate enzyme from papaya that mimics the activity of proteases secreted by helminth parasites. Depletion of basophils with antibody against FcεR1 diminishes the development of Th2 cells, suggesting that basophils are involved in Th2 cell differentiation. This study [39] strongly indicates that basophils are critically involved in Th2 responses by their unique function to produce early IL-4 and TSLP in response to papain or bromelain. It remains uncertain, however, whether basophil-derived IL-4 is indeed involved in the development of Th2 cells in response to stimuli other than protease allergens.

Basophils as Th2-inducing APC

Data from our group also supported a role of basophils in Th2 responses – we reported that IL-18 and IL-33 synergize with IL-3 to strongly induce basophil, but not mast cell, production of IL-4 and IL-13 *in vitro*, respectively [11, 12] (Fig. 1, left panel), suggesting a role of basophils in promoting Th2 response by producing IL-4. Furthermore, basophils are shown to be an important regulator of Th2 responses *in vivo*, particularly in helminth-infected mice [3, 15]. As the size of helminths is too large to be phagocytosed directly by DC, it is more likely that DC take up Ag shed or secreted by parasites and present the Ag on MHC class II complex to naïves T cells in the context of IL-4 from parasite Ag-stimulated basophils. Although this is a persuasive hypothesis, the exact role of basophils in Th2 development remains to be formally demonstrated.

As noted, three groups independently demonstrated that contrary to our intuition, DC are not required for the development of Th2 responses to protease allergens, helminthic parasites or complexes of Ag and IgE [36–38]. All three groups demonstrated that basophils express MHC class II, CD80/86 and produce IL-4. Two groups showed that basophils induce Th2 cells in the absence of DC [36, 38]. Our group demonstrated that administration of Ag-pulsed basophils but not Ag-pulsed DC or mast cells selectively induces Th2 cells *in vivo* [37] (Fig. 1, right panel). Together, the three studies [36–38] suggest that basophils induce allergen or helminth-induced Th2 response by functioning as Th2-inducing APC. Artis and colleagues [36], using MHC II^{CD11c} transgenic mice, where MHC class II expression is restricted to $CD11c^+$ DC, demonstrated that these mice, when inoculated with *T. muris*, fail to develop Th2 response and to expel helminths. MHC II^{CD11c} transgenic mice do not secrete intestinal goblet-specific immune effector molecule resistin-like molecule β, which is induced by Th2 cells. Artis and colleagues [36] simultaneously demonstrated that this infection induced the development of Th1 cells, suggesting that $CD11c^+$ cells are required for the generation of Th1 cells; basophils, on the other hand, are dominant Th2-inducing APC that express IL-4 and MHC class II, as supported by depletion of basophils *in vivo*, which led to impaired protective Th2 immunity to *T. muris* in wild-type

mice. Contrary to these findings, however, Min and colleagues [14] demonstrated that basophil depletion in *N. brasiliensis*-infected mice did not affect the development of Th2 cells, suggesting that *N. brasiliensis* infection induces Th2 immunity even in the absence of basophils. We therefore need further studies to reconcile this apparent discrepancy.

Medzhitov and colleagues [38] demonstrated that skin DC are dispensable for mounting Th2 responses to papain. This group previously reported that, as with injection of the soluble Ag of *S. mannsoni* eggs, papain rapidly induces recruitment of basophils to the lymph node [39]. In the lymph nodes, basophils secrete IL-4 and TSLP, which are critically involved in the development of Ag-specific Th2 cells. Given that this treatment simultaneously induced recruitment of DC, Medzhitov and colleagues [39] initially considered that basophils function as accessory cells and DC present Ag in the presence of IL-4 from basophils. In the follow-up study, Medzhitov and colleagues [38] very clearly demonstrated that skin DC are not required for the development of Th2 cells in the draining lymph nodes. In this study [38], papain was injected into the ear, where skin DC capture Ag and present Ag-derived peptides to naïve T cells in the draining lymph nodes. If skin DC capture Ag and present it at the lymph node, rapid removal of this Ag-pulsed DC by prompt excision of the injection site should inhibit the Th2 response; however, this treatment failed to inhibit development of Th2 cells, suggesting that Ag capture by skin DC is not required for induction of papain-specific Th2 development. Instead, soluble papain can directly enter lymph nodes from injection site. Furthermore, selective depletion of $CD11c^+$ DC did not inhibit Th2 development to papain, although mice failed to develop Th1 responses. Artis's [36] and Medzhitov's [38] groups used the same strategy to deplete DC, using the CD11c-restricted diphteria toxin receptor mice, in which CD11c-expressing DC are efficiently depleted upon delivery of diphteria toxin, the two groups demonstrated that DC depletion only inhibited the development of Th1 cells without affecting the development of Th2 response. These results strongly indicated that other type/s of APC might be required for Th2 cytokine-dependent immune response. Medzhitov's group [38] demonstrated that OVA-pulsed basophils induce the development of OVA-specific naïve $CD4^+$ T cells into Th2 cells *in vitro*. They also show basophils can uptake, process and present soluble Ag. They further demonstrated that adoptive transfer of OVA-pulsed basophils induced Th2 response in MHC class II-deficient mice.

Basophils produce IL-4 and IL-13 upon stimulation with Ag/IgE complex. In addition, our *in vitro* studies demonstrated that, among mast cells and basophils, only basophils strongly produce IL-4 and IL-13 in response to IL-3 and IL-18 or IL-33 [11, 12]. These data suggest a role of basophils in the development of Th2 cells. These observations led us to examine the possibility whether basophils directly induce the development of Th2 cells, instead of functioning as accessory cells *in vitro* [37].

Splenic basophils from mice inoculated with *S. venezuelensis* produce large amounts of IL-4, IL-6 and IL-13 in the medium even in the absence of exogenous IL-3. In contrast, splenic basophils from naïve mice produce small amounts of IL-4, IL-6 and IL-13 only in IL-3-containing medium. Furthermore, basophils from infected mice express MHC class II and strongly induce the development of OVA-specific naïve $CD4^+$ T cells into Th2 cells *in vitro* in the presence of OVA peptide, IL-2 and IL-3 without IL-4 (neutral culture condition). Thus, we initially regarded only basophils from infected mice as potent APC; however, we soon found that splenic basophils from naïve mice also express comparable level of MHC class II and have the capacity to strongly induce the development of Th2 cells *in vitro* under neutral conditions [37]. We next examined bone marrow basophils and showed that these also have the potential to induce the development of Th2 cells. We purified basophils from bone marrow cells cultured with IL-3 for 10 days. Similar to splenic basophils, bone marrow basophils express MHC class II, CD80, CD86 and CD62L. Furthermore, bone marrow basophils can take-up and process protein Ag and express peptide in association with MHC class II. In particular, bone marrow basophils can efficiently uptake a low dose of Ag/IgE complex, and present Ag/MHC class II and produce IL-4, suggesting that they are potent Th2-inducing APC.

We also demonstrated that i.v. administration of OVA-pulsed basophils, which we prepared by culturing basophils with DNP–OVA and anti-DNP–IgE complexes, strongly induce OVA-specific Th2 cells in the spleen of naïve mouse (Fig. 1, right panel). We found that basophils' APC activity was enhanced when pulsed with DNP-OVA in the presence of anti-DNP IgE. In contrast, i.v. administration of OVA-pulsed DC failed to induce Th2 cells, although this treatment induced IFN-γ-producing Th1 cells. Thus, basophils are potent Th2-inducing APC *in vivo*. We transferred only $0.25–0.5 \times 10^6$ basophils and found dramatic induction of Th2 responses. We have also demonstrated that single i.v. administration of low-dose DNP–OVA/anti-DNP–IgE complex into naïve mice rapidly and preferentially induced OVA-specific Th2 cells in an endogenous basophil-dependent manner. Such sensitized mice promptly produced OVA-specific IgG1 antibody in response to i.v. administration of soluble OVA. Furthermore, IL-3 treatment prepares mice to be highly susceptible to Th2-inducing action of IgE complex by increasing the number of basophils.

Clinical implication: Basophils as a potential therapeutic target

Animals respond to allergen exposure by producing Ag-specific IgE. Such sensitized individuals, upon re-exposure to the same allergens, increase the production of IgE, which form allergen–IgE complexes by binding to allergens. These IgE complexes are captured by basophils that develop into Th2-inducing APC and present allergen-derived peptide with MHC class II and provide IL-4 to naïve $CD4^+$ T cells. Thus, basophils play a very important role in amplification of Th2-IgE responses, suggesting that they may be an important therapeutic target and depletion of basophils by antibody such as anti-FcεR1 might be an effective

therapeutic pathway. Published work has suggested that anti-IgE therapy is effective for Th2-IgE diseases [40]. The effect of anti-IgE therapy is believed to interfere with IgE-mediated activation of mast cells and basophils; however, on the basis of our research, another consequence of this antibody therapy might be the inhibition of basophil development into Th2-inducing APC, adding another rationale for anti-IgE therapy.

Concluding remarks

Basophils can uptake intact proteins and process them into peptides. Thus, basophils have the potential to induce primary Th2 response (Fig. 2). FcεR1 has a dominant effect during the memory phase of the Th2 response, because FcεR1 has the capacity to bind a very small amount of Ag–IgE complex and to present Ag-derived peptide with MHC class II. Denzel *et al.* [41, 42] reported that basophils bind large amounts of intact Ag *via* FcεR1-bound IgE. These basophils activate $CD4^+$ T cells to enhance Ag-specific B-cell memory responses (proliferation and Ig production) by presenting Ag and secretion of IL-4 and IL-6, suggesting that activated basophils induce and activate Th2-type cells, which help B cell proliferation and IgG1 production.

Atopic individuals are characterized by increased number of basophils at sites of allergic inflammation [43–45]. Although human mature basophils lack HLA-DR, we have demonstrated that some of them re-express HLA-DR when stimulated with IL-3 [37]. Given that IL-3 and other factors may be present at high concentrations at the site of allergic inflammation, accumulated basophils might re-express HLA-DR. Once the immune system of individuals with atopy start to produce Ag-specific IgE, they can steadily increase the amounts Ag and Ag-specific IgE complex. This allows basophils to take up Ag–IgE complex and become potent Th2 cell-inducing APC and induce progressive allergic inflammation in these individuals. Antibody therapy against IgE or basophils might be effective, because depletion of IgE or basophils could diminish basophil-dependent induction of Th2 cells.

Acknowledgements: Supported by The Japanese Ministry of Education, Culture, Sports, Science and Technology (Grant-in-Aid for Scientific Research on Priority Areas 18073016 and Hitech Research Center Grant)

Conflict of interest: The author declares no financial or commercial conflict of interest.

References

1 Galli, S. J., Grimbaldeston, M. and Tsai, M., Immunomodulatory mast cells: negative, as well as positive, regulators of immunity. *Nat. Rev. Immunol.* 2008. 8: 478–486.

2 Galli, S. J., Kalesnikoff, J., Grimbaldeston, M. A., Piliponsky, A. M., Williams, C. M. and Tsai, M., Mast cells as "tunable" effector and immunoregulatory cells: recent advances. *Annu. Rev. Immunol.* 2005. 23: 749–786.

3 Min, B., Basophils: what they 'can do' versus what they 'actually do'. *Nat. Immunol.* 2008. 9: 1333–1339.

4 Karasuyama, H., Mukai, K., Tsujimura, Y. and Obata, K., Newly discovered roles for basophils: a neglected minority gains new respect. *Nat. Rev. Immunol.* 2008. 9: 9–13.

5 Sullivan, B. M. and Locksley, R. M., Basophils: a nonredundant contributor to host immunity. *Immunity* 2009. 30: 12–20.

6 Arinobu, Y., Iwasaki, H., Gurish, M. F., Mizuno, S., Shigematsu, H., Ozawa, H., Tenen, D. G. *et al.*, Developmental checkpoints of the basophil/mast cell lineages in adult murine hematopoiesis. *Proc. Natl. Acad. Sci. USA* 2005. 102: 18105–18110.

7 Saini, S. S., Klion, A. D., Holland, S. M., Hamilton, R. G., Bochner, B. S. and Macglashan, D. W., Jr., The relationship between serum IgE and surface levels of FcepsilonR on human leukocytes in various diseases: correlation of expression with FcepsilonRI on basophils but not on monocytes or eosinophils. *J. Allergy Clin. Immunol.* 2000. 106: 514–520.

8 Lantz, C. S., Yamaguchi, M., Oettgen, H. C., Katona, I. M., Miyajima, I., Kinet, J. P. and Galli, S. J., IgE regulates mouse basophil Fc epsilon RI expression *in vivo*. *J. Immunol.* 1997. 158: 2517–2521.

9 Yamaguchi, M., Lantz, C. S., Oettgen, H. C., Katona, I. M., Fleming, T., Miyajima, I., Kinet, J. P., Galli, S. J., IgE enhances mouse mast cell Fc(epsilon)RI expression *in vitro* and *in vivo*: evidence for a novel amplification mechanism in IgE-dependent reactions. *J. Exp. Med.* 1997. 185: 663–672.

10 Hida, S., Yamasaki, S., Sakamoto, Y., Takamoto, M., Obata, K., Takai, T., Karasuyama, H. *et al.*, Fc receptor gamma-chain, a constitutive component of the IL-3 receptor, is required for IL-3-induced IL-4 production in basophils. *Nat. Immunol.* 2009. 10: 214–222.

11 Yoshimoto, T., Tsutsui, H., Tominaga, K., Hoshino, K., Okamura, H., Akira, S., Paul, W. E. *et al.*, IL-18, although antiallergic when administered with IL-12, stimulates IL-4 and histamine release by basophils. *Proc. Natl. Acad. Sci. USA* 1999. 96: 13962–13966.

12 Kondo, Y., Kondo, Y., Yoshimoto, T., Yasuda, K., Futatsugi-Yumikura, S., Morimoto, M., Hayashi, N. *et al.*, Administration of IL-33 induces airway hyperresponsiveness and goblet cell hyperplasia in the lungs in the absence of adaptive immune system. *Int. Immunol.* 2008. 20: 791–800.

13 Yoshimoto, T. and Nakanishi, K., Roles of IL-18 in basophils and mast cells. *Allergol. Int.* 2006. 55: 105–113.

14 Kim, S., Prout, M., Ramshaw, H., Lopez, A. F., LeGros, G. and Min, B., Cutting edge: basophils are transiently recruited into the draining lymph nodes during helminth infection *via* IL-3, but infection-induced Th2 immunity can develop without basophil lymph node recruitment or IL-3. *J. Immunol.* 2010. 184: 1143–1147.

15 Min, B., Prout, M., Hu-Li, J., Zhu, J., Jankovic, D., Morgan, E. S., Urban, J. F., Jr. *et al.*, Basophils produce IL-4 and accumulate in tissues after infection with a Th2-inducing parasite. *J. Exp. Med.* 2004. 200: 507–517.

16 Ishikawa, Y., Yoshimoto, T. and Nakanishi, K., Contribution of IL-18-induced innate T cell activation to airway inflammation with mucus hypersecretion and airway hyperresponsiveness. *Int. Immunol.* 2006. 18: 847–855.

17 Schramm, G., Mohrs, K., Wodrich, M., Doenhoff, M. J., Pearce, E. J., Haas, H. and Mohrs, M., Cutting edge: IPSE/alpha-1, a glycoprotein from *Schistosoma mansoni* eggs, induces IgE-dependent, antigen-independent

IL-4 production by murine basophils *in vivo*. *J. Immunol.* 2007. 178: 6023–6027.

18 **Mukai, K., Matsuoka, K., Taya, C., Suzuki, H., Yokozeki, H., Nishioka, K., Hirokawa, K. *et al.***, Basophils play a critical role in the development of IgE-mediated chronic allergic inflammation independently of T cells and mast cells. *Immunity* 2005. 23: 191–202.

19 **Tsujimura, Y., Obata, K., Mukai, K., Shindou, H., Yoshida, M., Nishikado, H., Kawano, Y. *et al.***, Basophils play a pivotal role in immunoglobulin-G-mediated but not immunoglobulin-E-mediated systemic anaphylaxis. *Immunity* 2008. 28: 581–589.

20 **Zhu, J. and Paul, W. E.**, CD4 T cells: fates, functions, and faults. *Blood* 2008. 112: 1557–1569.

21 **Trinchieri, G.**, Interleukin-12 and the regulation of innate resistance and adaptive immunity. *Nat. Rev. Immunol.* 2003. 3: 133–146.

22 **Seder, R. A. and Paul, W. E.**, Acquisition of lymphokine-producing phenotype by CD4+T cells. *Annu. Rev. Immunol.* 1994. 12: 635–673.

23 **Korn, T., Bettelli, E., Oukka, M. and Kuchroo, K.**, IL-17 and Th17 cells. *Annu. Rev. Immunol.* 2009. 27: 485–518.

24 **Kimura, A. and Kishimoto, T.**, IL-6: Regulator of Treg/Th17 balance. *Eur. J. Immunol.* 2010. 40: 1830–1835.

25 **Sakaguchi, S., Yamaguchi, T., Nomura, T. and Ono, M.**, Regulatory T cells and immune tolerance. *Cell* 2008. 133: 775–787.

26 **Takeda, K., Kaisho, T. and Akira, S.**, Toll-like receptors. *Annu. Rev. Immunol.* 2003. 21: 335–376.

27 **Nakanishi, K., Yoshimoto, T., Tsutsui, H. and Okamura, H.**, Interleukin-18 is a unique cytokine that stimulates both Th1 and Th2 responses depending on its cytokine milieu. *Cytokine Growth Factor Rev.* 2001. 12: 53–72.

28 **Nakanishi, K., Yoshimoto, T., Tsutsui, H. and Okamura, H.**, Interleukin-18 regulates both Th1 and Th2 responses. *Annu. Rev. Immunol.* 2001. 19: 423–474.

29 **Amsen, D., Antov, A. and Flavell, R. A.**, The different faces of Notch in T-helper-cell differentiation. *Nat. Rev. Immunol.* 2009. 9: 116–124.

30 **Ito, T., Wang, Y. H., Duramad, O., Hori, T., Delespesse, G. J., Watanabe, N., Qin, F. X. *et al.***, TSLP-activated dendritic cells induce an inflammatory T helper type 2 cell response through OX40 ligand. *J. Exp. Med.* 2005. 202: 1213–1223.

31 **Aimanianda, V., Haensler, J., Lacroix-Desmazes, S., Kaveri, S. V. and Bayry, J.**, Novel cellular and molecular mechanisms of induction of immune responses by aluminum adjuvants. *Trends Pharmacol. Sci.* 2009. 30: 287–295.

32 **Anderson, C. F. and Mosser, D. M.**, A novel phenotype for an activated macrophage: the type 2 activated macrophage. *J. Leukoc. Biol.* 2002. 72: 101–106.

33 **Padigel, U. M., Hess, J. A., Lee, J. J., Lok, J. B., Nolan, T. J., Schad, G. A. and Abraham, D.**, Eosinophils act as antigen-presenting cells to induce immunity to *Strongyloides stercoralis* in mice. *J. Infect. Dis.* 2007. 196: 1844–1851.

34 **Oh, K., Shen, T., Le Gros, G. and Min, B.**, Induction of Th2 type immunity in a mouse system reveals a novel immunoregulatory role of basophils. *Blood* 2007. 109: 2921–2927.

35 **Hida, S., Tadachi, M., Saito, T. and Taki, S.**, Negative control of basophil expansion by IRF-2 critical for the regulation of Th1/Th2 balance. *Blood* 2005. 106: 2011–2017.

36 **Perrigoue, J. G., Saenz, S. A., Siracusa, M. C., Allenspach, E. J., Taylor, B. C., Giacomin, P. R., Nair, M. G. *et al.***, MHC class II-dependent basophil-CD4$^+$ T cell interactions promote Th2 cytokine-dependent immunity. *Nat. Immunol.* 2009. 10: 697–705.

37 **Yoshimoto, T., Yasuda, K., Tanaka, H., Nakahira, M., Imai, Y., Fujimori, Y. and Nakanishi, K.**, Basophils contribute to Th2-IgE responses *in vivo* via IL-4 production and presentation of peptide-MHC class II complexes to CD4$^+$ T cells. *Nat. Immunol.* 2009. 10: 706–712.

38 **Sokol, C. L., Chu, N. Q., Yu, S., Nish, S. A., Laufer, T. M. and Medzhitov, R.**, Basophils function as antigen-presenting cells for an allergen-induced T helper type 2 response. *Nat. Immunol.* 2009. 10: 713–720.

39 **Sokol, C. L., Barton, G. M., Farr, A. G. and Medzhitov, R.**, A mechanism for the initiation of allergen-induced T helper type 2 responses. *Nat. Immunol.* 2008. 9: 310–318.

40 **Adcock, I. M., Caramori, G. and Chung, K. F.**, New targets for drug development in asthma. *Lancet* 2008. 372: 1073–1087.

41 **Denzel, A. Maus, U. A., Rodriguez-Gomez, M., Moll, C., Nidermeier, M., Winter, C., Maus, R., *et al.***, Basophils enhance immunological memory responses. *Nat. Immunol.* 2008. 9: 733–742.

42 **Gauvreau, G. M., Lee, J. M., Watson, R. M., Irani, A. M., Schwartz, L. B., and O'Byrne, P. M.**, Increased numbers of both airway basophils and mast cells in sputum after allergen inhalation challenge of atopic asthmatics. *Am. J. Respir. Crit. Care Med.* 2000. 161: 1473–1478.

43 **Irani, A. M., Huang, C., Xia, H. Z., Kepley, C., Nafie, A., Fouda, E. D., Craig, S., *et al.***, Immunohistochemical detection of human basophils in late-phase skin reactions. *J. Allergy Clin. Immunol.* 1998. 101: 354–362.

44 **Koshino, T., Arai, Y., Miyamoto, Y., Sano, Y., Itami, M., Teshima, S., Hirai, K., *et al.***, Airway basophil and mast cell density in patients with bronchial asthma: relationship to bronchial hyperresponsiveness. *J. Asthma* 1996. 33: 89–95.

45 **Macfarlane, A. J., Kon, O. M., Smith, S. J., Zeibecoglou, K., Khan, L. N., Barata, L. T., McEuen, A. R., *et al.***, Basophils, eosinophils, and mast cells in atopic and nonatopic asthma and in late-phase allergic reactions in the lung and skin. *J. Allergy Clin. Immunol.* 2000. 105: 99–107.

Abbreviations: **BMCP:** basophils and mast cell precursor · **FcγR:** FcR common γ-chain · **GMP:** granulocyte/monocyte progenitor · **TSLP:** thymic stromal lymphopoetin

Full correspondence: Prof. Kenji Nakanishi, Department of Immunology and Medical Zoology, Hyogo College of Medicine, 1-1 Mukogawa-cho, Nishinomiya, Hyogo 663-8501 Japan
Fax: +81-798-40-5423
e-mail: nakaken@hyo-med.ac.jp

Received: 16/4/2010
Revised: 17/5/2010
Accepted: 18/5/2010

Hepatology Research

Hepatology Research 2010; 40: 823–831

doi: 10.1111/j.1872-034X.2010.00670.x

Original Article

Crucial role of impaired Kupffer cell phagocytosis on the decreased Sonazoid-enhanced echogenicity in a liver of a nonalchoholic steatohepatitis rat model

Shohei Yoshikawa,[1] Hiroko Iijima,[1] Masaki Saito,[1] Hironori Tanaka,[1] Hiroyasu Imanishi,[1] Naoki Yoshimoto,[2] Tomohiro Yoshimoto,[3] Shizue Futatsugi-Yumikura,[4] Kenji Nakanishi,[4] Tohru Tsujimura,[5] Takashi Nishigami,[5] Atsushi Kudo,[6] Shigeki Arii[6] and Shuhei Nishiguchi[1]

[1]*Division of Hepatobiliary and Pancreatic Diseases, Department of Internal Medicine, Hyogo College of Medicine,* [2]*Ultrasound Imaging Center, Hyogo College of Medicine,* [3]*Laboratory of Allergic Diseases, Institute for Advanced Medical Sciences, Hyogo College of Medicine,* [4]*Department of Immunology and Medical Zoology, Hyogo College of Medicine,* [5]*Department of Pathology, Hyogo College of Medicine, and* [6]*Department of Hepatobiliary Pancreatic Surgery, Tokyo Medical and Dental University, Tokyo, Japan*

Aims: To evaluate the dynamics of Kupffer cell (KC) phagocytosis by performing both *in vivo* and *in vitro* studies using Sonazoid (GE Healthcare, Oslo) in a rat nonalcoholic steatohepatitis (NASH) model.

Methods: Contrast enhanced ultrasonography (CEUS) was performed on a rat NASH model induced by a methionine choline deficient diet (MCDD) and control rats, and Sonazoid was used to measure the signal intensity in the liver parenchyma. The uptake of Sonazoid by the KCs was observed by intravital microscopy. Their phagocytic capability was evaluated *in vitro* using isolated and cultured KCs. The uptake of fluorescein isothiocyanate (FITC)-labeled latex beads was observed and quantitatively analyzed by flow cytometry.

Results: In the MCDD group, liver parenchymal enhancement was reduced 20 min after the Sonazoid injection. Microscopic observation of the isolated and cultured KCs revealed that the number of phagocytosed Sonazoid microbubbles was significantly decreased. Confocal laser scanning microscopic (CLSM) observation showed a decrease in the uptake of the latex beads. A decreased phagocytic capacity in the MCDD group was suggested by the quantitative analysis using flow cytometry, as well as by intravital microscopy.

Conclusions: CEUS with Sonazoid is a powerful evaluation tool to diagnose NASH from an early stage of the disease.

Key words: Kupffer cells, nonalcoholic steatohepatitis, phagocytosis, Sonazoid, ultrasound contrast agents.

INTRODUCTION

NONALCOHOLIC FATTY LIVER disease (NAFLD) has been increasing as the incidence of obesity and metabolic syndrome has been rising. Nonalcoholic steatohepatitis (NASH) draws particular attention due to the risk of progression to cirrhosis and hepatocellular carcinoma.[1–3] Liver biopsy has been considered to be the only way to definitively diagnose NASH[4,5] because diagnosis using imaging modalities is believed to be impossible.[6] In a recent study, magnetic resonance imaging was used for the quantification of the liver fat content and the evaluation of hepatic fibrosis, but it was still inadequate to replace liver biopsy.[7] Liver biopsy is not necessarily recommended for all NAFLD patients because of the risks of the procedure.

We have previously reported the usefulness of contrast enhancement ultrasound (CEUS) in the diagnosis of NASH with a contrast agent, Levovist, which is phagocytosed by the Kupffer cells (KC) in the liver.[8,9] In the liver parenchyma of NASH patients, the accumulation of Levovist microbubbles decreased remarkably 5 min after Levovist injection (especially by 20 min).

Correspondence: Dr Hiroko Iijima, Division of Hepatobiliary and Pancreatic Diseases, Department of Internal Medicine, Hyogo College of Medicine, 1-1 Mukogawa-cho, Nishinomiya, Hyogo 663-8501, Japan. Email: hiroko-i@hyo-med.ac.jp

Received 15 January 2009; revision 17 February 2010; accepted 19 January 2010.

Tsujimoto *et al.* demonstrated reduced contrast effect and phagocytic activity *in vitro* in a rat model prepared by a choline-deficient l-amino acid-defined (CDAA) diet.[10] However, they did not prove it *in vivo* in a rat model that the decreased parenchymal enhancement with Levovist was attributed to phagocytosis by KCs. Sonazoid (GE Healthcare, Oslo) has also been proven to be phagocytosed by KCs.[11,12] We performed CEUS using Sonazoid on a rat NASH model prepared by a methionine choline deficient diet (MCDD)[13] to evaluate the parenchymal enhancement. The phagocytosis of Sonazoid by phagocytic cells was observed *in vivo* in real time by intravital microscopy. To evaluate and prove Sonazoid phagocytosis *in vitro*, isolated and cultured KCs were observed and compared between the MCDD and control groups. Moreover, to evaluate the phagocytic capacity of KCs, the uptake of fluorescein isothiocyanate (FITC)-labeled latex beads was observed and a quantitative analysis was performed using flow cytometry.

METHODS

Animals

THIS STUDY PROTOCOL was approved by the Animal care committee of the Hyogo College of Medicine, and was performed in conformity with their institutional guidelines.

Male Wistar rats (190–200 g; SLC Japan, Tokyo), were housed in the animal facility of the Hyogo College of Medicine and kept at a controlled temperature of 23 ± 1 2°C under 12 h light/12 h dark cycles. Animals for the NASH model were given free access to tap water and MCDD (Oriental Yeast, Tokyo). Animals in the control group had free access to tap water and a normal laboratory diet (MF diet; Oriental Yeast). Animals on the 2nd, 4th and 8th weeks of the diet were used. For observation by intravital microscopy, 25% urethane (Wako Pure Chemical Industries, Osaka) subcutaneous anesthesia was used; and for other observations, isoflurane (Takeda Pharmaceutical, Tokyo) inhalation anesthesia was used.

Histological examination

The liver tissues were fixed in 10% formalin, and then stained with hematoxylin and eosin or Azan. Then, the degree of steatosis, inflammation and fibrosis were assessed from the tissues using the Brunt's histological grading and scoring system.

Preparation of contrast agents and latex beads

The contrast agent Sonazoid and 2.6% FITC-labeled latex beads (Polyscience, Warrington, PA) with diameters of 1 m and 2 m, were used. They were diluted with distilled water to 1 10^9 microbubbles/mL and 1 10^9 beads/mL, respectively.

Contrast enhanced ultrasound using Sonazoid

Sonazoid at 0.015 L (approximately 1.5 10^4 microbubbles)/100g body was injected into the caudal vein after being diluted with distilled water to a total volume of 500 L.

CEUS was performed by a Toshiba Aplio (Toshiba Medical Systems, Tokyo) with a 7.5 MHz linear transducer. Following conventional B-mode imaging, images were obtained in Advanced Dynamic Flow (ADF) mode with a high mechanical index (MI) of 1.0 to cause destructions of the Sonazoid bubbles. The images were obtained at a focus depth of 3 cm from the body surface at a frame rate of 10 frames/second.

Scanning was performed in various planes of the liver at 20 and 50 min after the Sonazoid injection. This scanning time was based on evidence that the Kupffer phase started at approximately 20 min after the Sonazoid injection when the washout of Sonazoid from the hepatic vein was observed in a healthy volunteer.[14] On the 2nd, 4th, and 8th weeks of the diet, CEUS was performed on four animals from each group to see if any differences in parenchymal enhancement could be detected depending on the duration of the diet. CEUS using ADF was performed at 20 min after the Sonazoid injection to measure the parenchymal intensity within the region of interest (ROI), which was randomly set in the depth within the focus area. The average signal intensity in the liver parenchyma was then calculated after it was converted to sound pressure using the antilog calculation. Scanned images were recorded separately as ADF signals and gray scale signals.

Intravital microscopic observation of phagocytosis by Kupffer cells

Animals in both groups were opened under anesthesia to expose their livers, and were placed in a prone position on a 3 cm diameter transplant platform. A 23 gauge indwelling cannula was inserted into the caudal vein, and 500 L of 150 L/100 g Sonazoid diluted with distilled water was administered.

Preparation and phagocytosis of Kupffer cells – *in vitro* study

KCs were isolated from animals in both groups with the previously published procedure: After anesthetizing the animals by isofluran inhalation, the portal vein was cannulated with a 20-gauge needle and the inferior vena cava was opened and a perfusion circuit was created.

Briefly, liver non-parenchymal cells were isolated by the pronase-collagenase method as previously described,[15] and eluted fractions were collected using a Beckman J6-MC centrifuge (Beckman Coulter, Fullerton, CA). The cells were washed, and re-suspended in Roswell Park Memorial Institute (RPMI) 1640 supplemented with 10% fetal bovine serum containing 2-ME (50 M), L-glutamine (2 mM), penicillin (100 U/mL) and streptomycin (100 g/mL), plated onto plastic dishes 3.5 cm in diameter, and incubated for 24 h. The plastic adherent cells (1 10^6/mL) were then incubated with 3 10^5 Microbubble/ml Sonazoid for 30 min. After washing the plates with culture medium, the uptake of Sonazoid by the isolated KCs was observed by inverted microscopy (TE300-HM-2; Nikon, Tokyo) in a micro-incubator at 37°C in 5% CO_2. The microscopic images were recorded by image analyzing software (Aquacosmos; Hamamatsu Photonics, Shizuoka). The Sonazoid microbubbles phagocytosed by the KCs were then counted.

Observation of phagocytosis by Kupffer cells – *in vivo* study

Confocal laser scanning microscopy (CLSM)

Latex beads (diameter: 2 m, concentration: 1 10^8/kg) were administered through the caudal vein of animals from both groups. At 60 min after injection, the animals were sacrificed by anesthesia overdose to prepare frozen sections of the liver. The frozen sections were observed by CLSM (LSM510; Carl Zeiss, Jena).

Flow cytometric quantitative analysis of phagocytic capacity of Kupffer cells

Prior to the experiment, we determined the gating area of KCs fraction using purified KCs according to their forward scatter (FSC) and side scatter (SSC) on a flow cytometer. Once the gated area for KCs was determined, it was used for the rest of the experiments. Aliquots of 1 10^8/kg of FITC-labeled latex beads (diameters: 1 m and 2 m) were injected in both groups. At 1 h after injection, KCs isolated by the above-mentioned procedure were cultured for 24 h in an incubator at 37°C in 5% CO_2 to purify the KC fraction and reduce the contaminated cells. Following several washes with phosphate buffered saline (PBS), KCs adhered to the bottom of the dishes were detached with 0.25% Trypsin ethylenediaminetetraacetic acid (EDTA; Invitrogen, Tokyo). They were then centrifuged, and RPMI was added to the sediment to make a total volume of 1 mL in a culture tube. KCs in the tube were then analyzed by flow cytometry. The equipment used was a FACScan (BD Bioscience, San Jose, CA).

Statistics

The statistical significance of the signal intensity change in both groups was evaluated using a repeated measures analysis of variance (ANOVA) test. The Kruskal–Wallis test and Scheffe's *F*-test were performed for a comparison of the phagocytic capacity of isolated and cultured KCs between both groups. All data were analyzed by a statistical software package (SPSS, Chicago, IL).

RESULTS

Changes in liver histology

THE HISTOLOGICAL CHANGES were found as follows: the MCDD-2wk group revealed inflammation and steatosis, but no fibrosis. The MCDD-4wk group showed inflammation, steatosis and slight fibrosis, which was equivalent to grade 2/stage 2 of Blunt's grading/staging system. Inflammation and steatosis were found in the MCDD-8wk group, and their fibrosis was more severe than the one in the MCDD-4wk group, and was corresponding to Blunt's grade 2 /stage 3.

Sonazoid CEUS examination

The signal intensity decreased after Sonazoid injection in the MCDD group as compared to the control group. The quantification of the signal intensity at 20 min after injection is shown in Figure 1. The parenchymal intensity in the control group was 5.0 and 5.5 at 20 and 50 min after Sonazoid injection, respectively, but was 13.0 and 13.3 in the MCDD-4wk group, respectively. In the control group, the intensity decreased slightly to 3.5dB, 4.8dB and 5.5dB on the 2nd, 4th and 8th weeks of administration, respectively. In contrast, in the MCDD group, the intensity decreased according to the duration of the diet administration as to 11.5dB, 13.0dB and 20.5dB on the 2nd, 4th and 8th weeks, respectively; this was a significant difference between the groups ($P < 0.05$) (Figs 1,2).

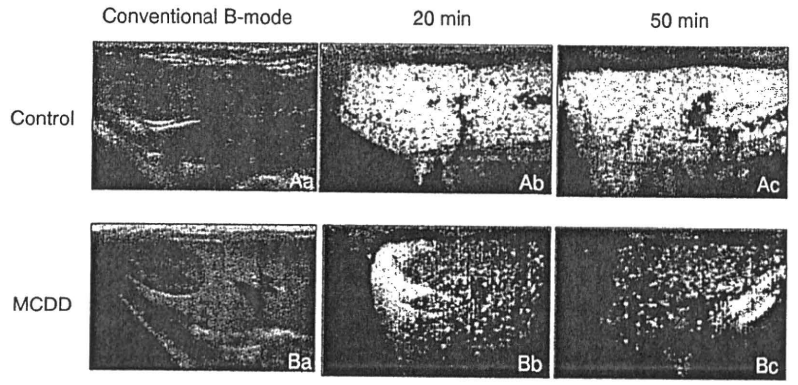

Figure 1 Abdominal US B-mode images (Aa, Ba) and Sonazoid CEUS images (Ab, Ac, Bb, Bc) of control rats (Aa-c) and MCDD-4wk fed rats (Ba-c). The hepato-renal echo contrast was greater in the MCDD rat group as compared with the control group. The livers in the control rats were clearly enhanced until 50 min after injection. In contrast, the enhancement of the liver decreased in the MCDD rats at both 20 and 50 min after injection.

Time course change of Sonazoid phagocytosis observed by intravital microscopy

Five animals from each group were compared. Particles appeared on the sinusoidal wall were observed almost simultaneously at Sonazoid administration, and then the uptake of Sonazoid by phagocytic cells on the sinusoidal wall was recorded using a fixed camera in the view area of the portal vein before Sonazoid injection until 30 min after injection (Fig. 3). The time course was observed by intravital microscopy for 30 min after the Sonazoid injection, and showed that the number of Sonazoid microbubbles phagocytosed by the KCs kept increasing in the control group. However, in the MCDD group, only several Sonazoid microbubbles were phagocytosed by the KCs (Fig. 4).

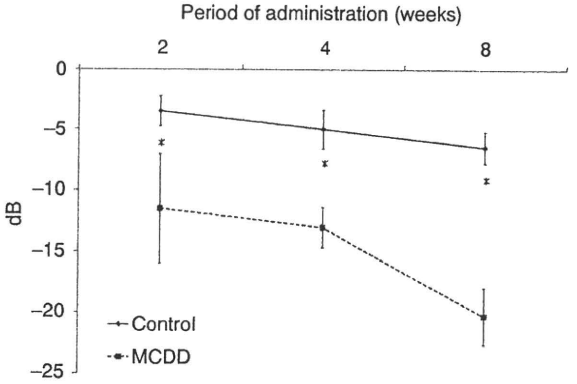

Figure 2 Liver parenchymal intensity (dB) of Sonazoid CEUS on control and MCDD rats at 2 weeks, 4 weeks and 8 weeks of diet administration. The vertical axis is the signal intensity (dB) and the horizontal axis is the duration of diet administration. The parenchymal intensity in the MCDD group showed a decrease as compared with the control group at 11.5dB, 13dB and 20.5dB at the 2nd, 4th, and 8th weeks after administration, respectively ($P < 0.05$).

Phagocytosis of FITC-labeled latex beads by Kupffer cells – *in vivo*

CLSM observations

The number of FITC-labeled latex beads phagocytosed by the KCs and stained as fluorescent green was compared between the two groups. The number of fluorescent-green phagocytosed latex beads in the MCDD group decreased in comparison with the control group, and this suggested decreased phagocytic capacity of the Kupffer cells in the MCDD group (Fig. 5).

Phagocytosis of isolated Kupffer cells – *in vitro*

The inverted microscopic observation of isolated and cultured KCs with Sonazoid is shown in Figure 6. Significant differences were found between the control group and each week of the MCDD groups, and also between the MCDD-2wk and MCDD-8wk groups and between the MCDD-4wk and MCDD-8wk groups ($P < 0.01$) (Fig. 6).

Phagocytosis capability by flow cytometric analysis

Flow cytometric analysis was performed to quantify the phagocytic capacity of isolated and cultured KCs, which were treated with fluorescent latex beads. The phagocytosis rate in the control group was 88%, and many latex beads were ingested. In contrast, the rate was 61% in the MCDD-2wk (B), 37% in the MCDD-4wk (C) and 27% in the MCDD-8wk (D) groups, where the phagocytic capacity had decreased in proportion to the duration

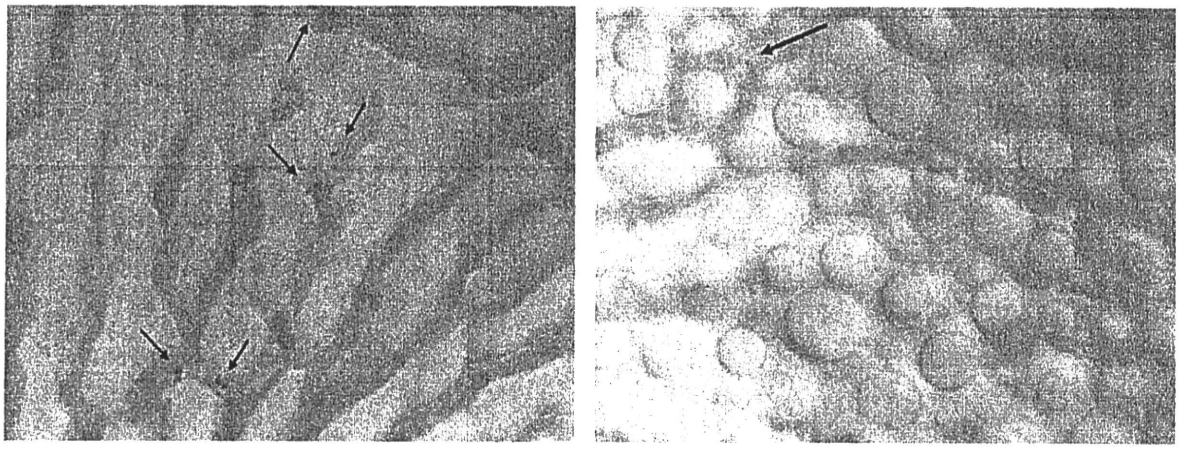

Figure 3 Intravital microscopic observation at 30 min after Sonazoid injection. A number of Sonazoid were phagocytosed by phagocytic cells in the control group; whereas a couple of them were phagocytosed in the MCDD-2wk group.

of the MCDD administration. The phagocytosis index (expressed by the number of KCs which phagocytosed beads/the total number of KCs) in the MCDD group was also lower than in the control groups at every duration of the MCDD administration (Fig. 7). This finding revealed that the phagocytic capacity started to decrease at the early stages of the disease, and kept on decreasing week by week.

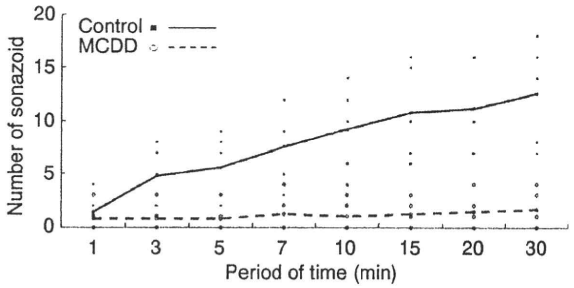

Figure 4 Time-course change in the phagocytosis of Sonazoid. The number of Sonazoid microbubbles phagocytosed by the KCs was plotted at 1, 3, 5, 7, 10, 15, 20 and 30 min after the Sonazoid injection. The control group is shown with a solid line and the MCDD-2wk group is shown with a broken line. Significant difference was seen in the two groups ($P < 0.001$). In the control group, the phagocytosis of Sonazoid increased up to 30 min after Sonazoid injection. In the MCDD-2wk group, only a couple of Sonazoid microbubbles were phagocytosed over a couple min after the injection.

DISCUSSION

NASH HAS BEEN increasing worldwide, and is the most common form of non-alcoholic/non-viral liver disease in the United States and European countries.[16] NAFLD was once considered a benign, reversible condition, and therefore was often left untreated. However, since NASH was introduced by Ludwig, a strong risk of this disease progressing to cirrhosis and hepatocellular carcinoma has been identified.[1–3] In the United States, an estimate shows about 30% of the population has NAFLD, and about 10% of these NAFLD patients has NASH.[17] In countries other than the United States, many people are believed to be developing NASH as their diets become Westernized.[18]

Ultrasonography is used for various organs as a non-invasive diagnostic modality. Ultrasound diagnosis with an intravenous contrast agent is also widely used, and has become indispensable especially in diagnosing the liver diseases.[19,20] The sonographic features of NAFLD including NASH are a high-level echo, a bright liver, vascular blurring, deep attenuation and hepatorenal contrast.[21–24] Abdominal computerized tomography (CT), which provides a more objective assessment, diagnoses NAFLD when the liver to spleen ratio (L/S ratio) is less than 0.9.[25] Thus, the diagnosis of NAFLD could be easily made by these imaging modalities, although distinguishing NASH from NAFLD is considered to be difficult by means of only imaging modalities and blood tests or an invasive liver biopsy is

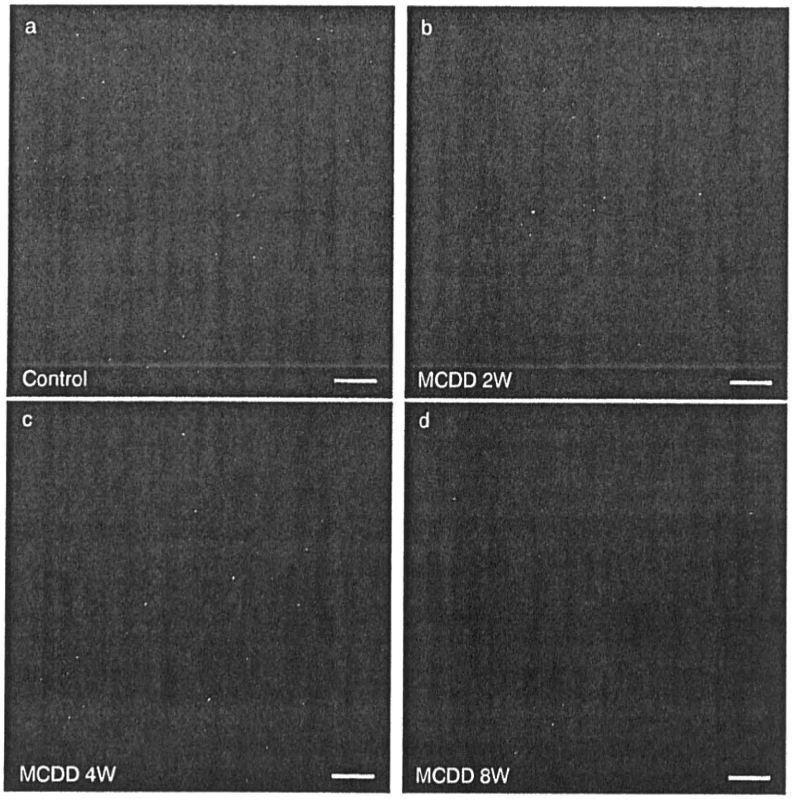

Figure 5 The animals were sacrificed at 60 min after fluorescent latex beads injection and were observed by CLSM. Many latex beads were observed in the control rats (shown in A) as compared with the MCDD rats (in B-D). The fluorescent agent of the latex beads is recognized as green.

required.[4–6] Given the prevalence of NAFLD patients, which has been reported to be as high as 30% of adults who get a medical checkup,[4–6] establishing non-invasive and reliable methods for diagnosing NASH is urgently needed. In the past, we have reported the usefulness of CEUS diagnosis using Levovist to distinguish NASH from NAFLD[9] because it is not realistic to perform liver biopsies for so many NAFLD patients. The diagnosis is made possible by the fact that the liver parenchymal enhancement significantly decreases in NASH patients at 20 min after Levovist injection during the delayed parenchymal phase. One suspected reason for this is the decreased phagocytic capacity of KCs in NASH.[9] Levovist was proven to be phagocytosed by KCs.[11] Furthermore, a study using latex beads on a rat NASH model prepared by a CDAA diet also showed reduced KC phagocytic function, with no changes in the KC numbers, in which the decreased parenchymal contrast effect was possibly attributed to a decrease in the phagocytic capability of KCs, although it did not prove that Levovist itself was phagocytosed by KCs.[10] Moreover, a recent study reported that the engulfment of erythrocytes by KCs was observed by electron microscopy in a rat NASH model induced by a high-fat diet.[26]

Sonazoid is a microbubble with a diameter of 2–4 m, and contains perfulbutane gas. It has a phospholipid shell which is negatively charged on its surface, and is known to be phagocytosed by liver macrophages, the KCs.[27,28] A report showed that 99% of Sonazoid and 47% of Levovist microbubbles were phagocytosed by isolated and cultured rat KCs;[11] In other words, Sonazoid is expected to be more readily phagocytosed than Levovist. In the present study, the time-course change of KC phagocytosis was investigated by performing CEUS on both MCDD and control rats using Sonazoid by intravital microscopy, and by analyzing isolated and cultured KCs. Sonazoid CEUS performed on a rat NASH model at 20 and 50 min after Sonazoid injection showed a significant decrease in enhancement at 50 min (Fig. 1). Using intravital microscopic observation, the Sonazoid continued to be phagocytosed in the control group, whereas in the MCDD group, the number of phagocytosed Sonazoid

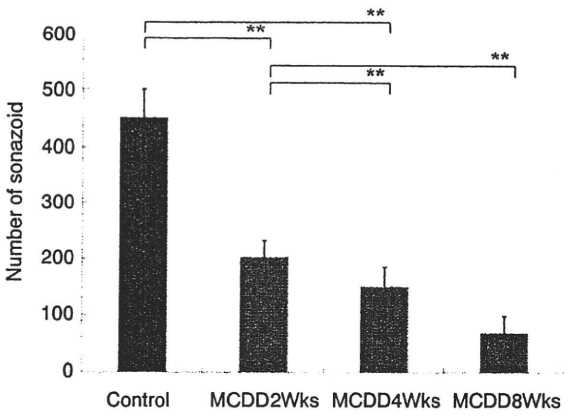

Figure 6 The number of Sonazoid microbubbles phagocytosed by isolated KCs in the control group and the MCDD-2wk, 4wk and 8wk groups were observed by inverted microscopy. After Sonazoid was added, the isolated KCs were cultured before observation. The number of Sonazoid microbubbles phagocytosed by 10 KCs in the control group was 450.5 ± 48.5, whereas 204.1 ± 28.7, 150.9 ± 34.2, and 69.7 ± 29.1 microbubbles were phagocytosed in the MCDD-2wk, 4wk and 8wk groups, respectively (mean ± standard deviation). Significant differences were found between the control group and each week of the MCDD groups, and also between the MCDD-2wk and MCDD-8wk groups and between the MCDD-4wk and MCDD-8wk groups ($P < 0.01$).

microbubbles by phagocytic cells was few after injection. Considering that most of phagocytic cells on sinusoidal wall are KCs, it is reasonable to think contrast agent is phagocytosed by KCs in hepatic sinusoids. Time-course observation also showed the number of phagocytosed microbubbles by phagocytic cells did not increase in the MCDD group (Fig. 4). This finding suggests that the phagocytic capability of KCs may start to decrease during the early stage of NASH, and that could enable the diagnosis of NASH at an early stage of fibrosis. To demonstrate these findings using isolated and cultured KCs, the number of phagocytosed Sonazoid microbubbles decreased in the MCDD rats (Fig. 6). In addition, the number of phagocytosed Sonazoid or latex beads tended to decrease in proportion to the duration of the MCDD administration (Fig. 5). In NASH patients, fibrosis is often detected at a late stage of the disease, because NASH is usually monitored as NAFLD. However, by using Sonazoid CEUS, the diagnosis of NASH could be possible at an early stage, and this represents a groundbreaking development in NASH treatment.

Our study also suggested the clinical usefulness of Sonazoid CEUS in the diagnosis of NASH by demonstrating that: (i) parenchymal enhancement was decreased in the delayed parenchymal phase; and (ii) the phagocytic capacity of Kupffer cells was lowered as the duration of MCDD administration increased. Considering that Sonazoid is specifically phagocytosed by Kupffer cells, the quantification of phagocytic capacity should also be possible.

Some studies have reported the narrowed sinusoids seen in steatosis and steahohepatitis disturb the hepatic microcirculation.[29–31] In particular, the sinusoidal space of a NAFLD animal model was reduced by up to 50 % of the size of healthy control animals.[31] In order to preclude the possibility that the lowered liver parenchymal enhancement was caused by a circulatory disturbance of the contrast agent, latex beads with a diameter of 1 m, which is smaller than the diameter of Sonazoid (2 m), were used in the present *in vivo* study, since the width of a normal sinusoid is approximately 5 m. We performed CEUS with Levovist (4 mL/body) at one minute after Levovist intravenous injection in the early vascular phase to see if decreased parenchymal enhancement was associated with the narrowed sinusoids. Additionally, the parenchymal enhancement of fatty liver patients, NASH patients and healthy volunteers at 1 min after Levovist injection showed a similar intensity in the liver parenchyma in the early vascular phase (Fig. 8). These results demonstrated that the decreased enhancement of liver parenchyma was not due to the narrowed sinusoids or circulatory disturbances.

As shown above, our results suggested decreased Sonazoid-enhanced echogenicity was mainly due to impaired KC phagocytosis, although narrowed sinusoids could be present in MCDD rats due to fatty liver. Sonazoid CEUS could become a useful tool to distinguish NASH patients from many NAFLD patients.

ACKNOWLEDGEMENTS

THIS STUDY WAS supported by a Grant-in-Aid for Scientific Research from the Ministry of Education, Culture, Sports, Science and Technology of Japan, nos. 19500428 and 21300194 and a Grant-in-Aid for Researchers, Hyogo College of Medicine.

We thank all of our colleagues in the Division of Hepatobiliary and Pancreatic Medicine, Ms Sayaka Fujii and Ms Mayumi Yamada, for providing support for our experiments, and the technicians in the Ultrasound Imaging Center.

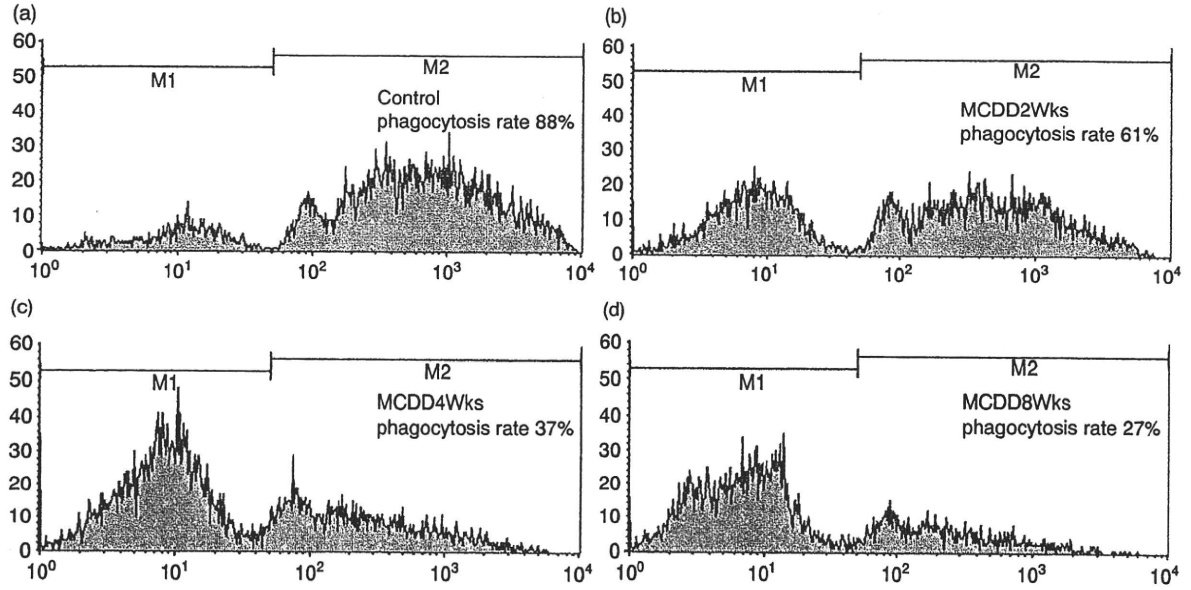

Figure 7 Flow cytometric analysis of isolated and cultured KCs after being treated with fluorescent latex beads. The vertical axis is the KC count and the horizontal axis is the fluorescent intensity. M1 is the number of KCs which did not phagocytose any beads, and M2 is the number of KCs which phagocytosed beads. The phagocytosis rate was calculated by M2/M1 + M2 (the total number of KCs). The phagocytosis rate in the control group was 88% and many latex beads were ingested, whereas the rate was 61 % in the MCDD-2wk (B), 37% in the MCDD-4wk (C) and 27% in the MCDD-8wk (D) groups, where the phagocytic capacity was decreased in proportion to the duration of MCDD administration.

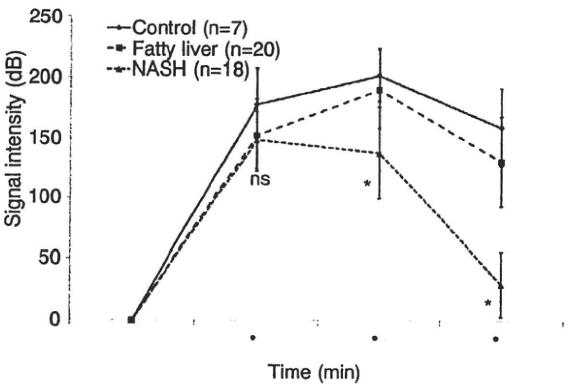

Figure 8 Parenchymal signal intensity in the early vascular phase and the delayed parenchymal phase of Levovist CEUS was evaluated in seven controls (healthy volunteers), 20 fatty liver patients and 18 NASH patients. At 1 min after the Levovist injection, the signal intensity was 178.1 ± 29.3 in the controls, 152.4 ± 30.0 in the fatty liver patients and 148.5 ± 23.6 in the NASH patients (mean ± standard deviation) and no significant differences were observed. However, at 5 and 20 min after injection, there was a significant decrease in the signal intensity in the NASH group.

REFERENCES

1 Ludwig J, Viggiano TR, McGill DB, Oh BJ. Nonalcoholic steatohepatitis: Mayo Clinic experiences with a hitherto unnamed disease. *Mayo Clin Proc* 1980; 55: 434–8.
2 Bugianesi E, Leone N, Vanni E *et al.* Expanding the natural history of nonalcoholic steatohepatitis: from cryptogenic cirrhosis to hepatocellular carcinoma. *Gastroenterology* 2002; 123: 134–40.
3 Shimada M, Hashimoto E, Taniai M *et al.* Hepatocellular carcinoma in patients with non-alcoholic steatohepatitis. *J Hepatol* 2002; 37: 154–60.
4 Saadeh S, Younossi ZM, Remer EM *et al.* The utility of radiological imaging in nonalcoholic fatty liver disease. *Gastroenterology* 2002; 123: 745–50.
5 Brunt EM, Janney CG, Di Bisceglie AM, Neuschwander-Tetri BA, Bacon BR. Nonalcoholic steatohepatitis: a proposal for grading and staging the histological lesions. *Am J Gastroentero* 1999; 94: 2467–74.
6 Matteoni CA, Younossi ZM, Gramlich T, Boparai N, Liu YC, McCullough AJ. Nonalcoholic fatty liver disease: a spectrum of clinical and pathological severity. *Gastroenterology* 1999; 116: 1413–9.
7 Schwenzer NF, Springer F, Schraml C, Stefan N, Machann J, Schick F. Non-invasive assessment and quantification of

liver steatosis by ultrasound, computed tomography and magnetic resonance. *J Hepatol* 2009; **51**: 433–5.
8 Iijima H, Moriyasu F, Miyahara T, Yanagisawa K. Ultrasound contrast agent, Levovist microbubbles are phagocytosed by Kupffer cells-In vitro and in vivo studies. *Hepatol Res* 2006; **35**: 235–7.
9 Iijima H, Moriyasu F, Tsuchiya K, Suzuki S, Yoshida M. Decrease in accumulation of ultrasound contrast microbubbles in non-alcoholic steatohepatitis. *Hepatol Res* 2007; **37**: 722–30.
10 Tsujimoto T, Kawaratani H, Kitazawa T *et al*. Decreased phagocytic activity of Kupffer cells in a rat nonalcoholic steatohepatitis model. *World J Gastroenterol* 2008; **14**: 6036–43.
11 Yanagisawa K, Moriyasu F, Miyahara T, Yuki M, Iijima H. Phagocytosis of ultrasound contrast agent microbubbles by Kupffer cells. *Ultrasound Med Biol* 2007; **33**: 318–25.
12 Watanabe R, Matsumura M, Munemasa T, Fujimaki M, Suematsu M. Mechanism of hepatic parenchyma-specific contrast of microbubble-based contrast agent for ultrasonography: microscopic studies in rat liver. *Invest Radiol* 2007; **42**: 643–51.
13 Weltman MD, Farrell GC, Liddle C. Increased hepatocyte CYP2E1 expression in a rat nutritional model of hepatic steatosis with inflammation. *Gastroenterology* 1996; **111**: 1645–53.
14 Sasaki S, Iijima H, Moriyasu F, Hidehiko W. Definition of contrast enhancement phases of the liver using a perfluoro-based microbubble agent. *Ultrasound Med Biol* 2009; **35**: 1819–27.
15 Tsutsui H, Mizoguchi Y, Morisawa S. Importance of direct hepatocytolysls by liver macrophages in experimental fulminant hepatitls. *Hepatogastroenterology* 1992; **39**: 553–9.
16 Skelly MM, James PD, Ryder SD. Findings on liver biopsy to investigate abnormal liver function tests in the absence of diagnostic serology. *J Hepatol* 2001; **35**: 195–9.
17 Green RM. NASH:hepatic metabolism and not simply the metabolic syndrome. *Hepatology* 2003; **38**: 14–7.
18 Charlton M. Nonalcoholic fatty liver disease: a review of current understanding and future impact. *Clin Gastroenterol Hepatol* 2004; **2**: 1048–58.
19 Harvey CJ, Blomley MJ, Eckersley RJ, Heckemann RA, Butler-Barnes J, Cosgrove DO. Pulse-inversion mode imaging of liver specific microbubbles: improved detection of subcentimetre metastases. *Lancet* 2000; **355**: 807–8.
20 Gaiani S, Celli N, Piscaglia F *et al*. Usefulness of contrast-enhanced perfusional sonography in the assessment of hepatocellular carcinoma hypervascular at spiral computed tomography. *J Hepatol* 2004; **41**: 421–6.
21 Taylor KJ, Carpenter DA, Hill CR, McCready VR. Gray scale ultrasound imaging. The anatomy and pathology of the liver. *Radiology* 1976; **119**: 415–23.
22 Joseph AE, Dewbury KC, McGuire PG. Ultrasound in the detection of chronic liver disease (the 'bright liver'). *Br J Radiol* 1979; **52**: 184–8.
23 Foster KJ, Dewbury KC, Griffith AH, Wright R. The accuracy of ultrasound in the detection of fatty infiltration of the liver. *Br J Radiol* 1980; **53**: 440–2.
24 Yajima Y, Ohta K, Narui T, Abe R, Suzuki H, Ohtsuki M. Ultrasonographical diagnosis of fatty liver: significance of the liver-kidney contrast. *Tohoku J Exp Med* 1983; **139**: 43–50.
25 Ricci C, Longo R, Gioulis E *et al*. Noninvasive in vivo quantitative assessment of fat content in human liver. *J Hepatol* 1997; **27**: 108–13.
26 Otogawa K, Kinoshita K, Fujii H *et al*. Erythrophagocytosis by liver macrophages (Kupffer cells) promotes oxidative stress, inflammation, and fibrosis in a rabbit model of steatohepatitis: implications for the pathogenesis of human nonalcoholic steatohepatitis. *Am J Pathol* 2007; **170**: 967–80.
27 Sontum PC, Ostensen J, Dyrstad K, Hoff L. Acoustic properties of NC100100 and their relation with the microbubble size distribution. *Invest Radiol* 1999; **34**: 268–75.
28 Sontum PC. Physicochemical characteristics of Sonazoid, a new contrast agent for ultrasound imaging. *Ultrasound Med Biol* 2008; **34**: 824–33.
29 Ijaz S, Yang W, Winslet MC, Seifalian AM. Impairment of hepatic microcirculation in fatty liver. *Microcirculation* 2003; **10**: 447–56.
30 McCuskey RS, Ito Y, Robertson GR, McCuskey MK, Perry M, Farrell GC. Hepatic microvascular dysfunction during evolution of dietary steatohepatitis in mice. *Hepatology* 2004; **40**: 386–93.
31 Farrell GC, Teoh NC, McCuskey RS. Hepatic microcirculation in fatty liver disease. *Anat Rec (Hoboken)* 2008; **291**: 684–92.

Hindawi Publishing Corporation
Gastroenterology Research and Practice
Volume 2010, Article ID 641865, 11 pages
doi:10.1155/2010/641865

Review Article

The TLR4/TRIF-Mediated Activation of NLRP3 Inflammasome Underlies Endotoxin-Induced Liver Injury in Mice

Hiroko Tsutsui,[1] Michiko Imamura,[1,2,3,4] Jiro Fujimoto,[2] and Kenji Nakanishi[3]

[1] *Department of Microbiology, Hyogo College of Medicine, 1-1, Mukogawa-cho, Nishinomiya 663-8501, Japan*
[2] *Department of Surgery, Hyogo College of Medicine, 1-1, Mukogawa-cho, Nishinomiya 663-8501, Japan*
[3] *Department of Immunology & Medical Zooloty, Hyogo College of Medicine, 1-1, Mukogawa-cho, Nishinomiya 663-8501, Japan*
[4] *Cancer Center, Hyogo College of Medicine, Nishinomiya, Japan*

Correspondence should be addressed to Hiroko Tsutsui, gorichan@hyo-med.ac.jp

Received 11 March 2010; Accepted 22 April 2010

Academic Editor: Ekihiro Seki

Administration of heat-killed *Propionibacterium acnes* renders mice highly susceptible to LPS. After LPS challenge *P. acnes*-primed mice promptly show hypothermia, hypercoagulation (disseminated intravascular coagulation), elevation of serum proinflammatory cytokine levels, and high mortality. The surviving mice develop liver injury. As previously reported, IL-18 plays a pivotal role in the development of this liver injury. Many cell types including macrophages constitutively store IL-18 as biologically inactive precursor (pro) form. Upon appropriate stimulation exemplified by TLR4 engagement, the cells secrete biologically active IL-18 by cleaving pro-IL-18 with caspase-1. Caspase-1 is also constitutively produced as a zymogen in macrophages. Recently, NLRP3, a cytoplasmic pathogen sensor, has been demonstrated to be involved in the activation of caspase-1. Here, we review the molecular mechanisms for the liver injuries, particularly focusing on the TLR4/NLRP3-mediated caspase-1 activation process, with a brief introduction of the mechanism underlying *P. acnes*-induced sensitization to LPS.

1. Introduction

TLR, topics of this issue, is an extracellular sensor family of pathogen-associated molecular patterns (PAMPs) [1, 2]. As described by Yamamoto et al. in this special issue, TLR1, TLR2, TLR4, TLR5, TLR6, and TLR11 are expressed on the cell surface, while TLR3, TLR7, TLR8, and TLR9 are expressed on the membrane of endosome, which is a transport vesicle originated from the cell membrane to trap and transport the extracellular macromolecules into the inside of the cells. Besides, mammalian host possess cytoplasmic sensors consisting of at least two families, RIG-I-like receptor (RLR) and Nod-like receptor (NLR) families [3–5]. After sensing intracellular, virus-derived double-stranded (ds) RNA, RLR members relay a signal to activate inflammatory responses for viral clearance via induction of proinflammatory cytokines and type 1 IFNs [6, 7]. Some of the NLR family members are associated with the cytoplasmic formation and activation of inflammasome. Inflammasome is a multiple protein complex and is regarded as the platform for activation of caspase-1 [8, 9]. Caspase-1 is produced as enzymatically inactive precursors (pro) and requires appropriate cleavage to become active. Macrophages including Kupffer cells constitutively produce procaspase-1 and accomplish caspase-1 activation in the inflammasomes after being stimulated [10–12]. Caspase-1 cleaves biologically inactive pro-IL-1β and pro-IL-18, leading to extracellular release of the corresponding active forms. Many cell types including Kupffer cells produce and store pro-IL-18 in the steady state, while they start to produce pro-IL-1β only after activation with appropriate stimuli [13–15]. Thus, the inflammasomes contribute to the secretion of IL-18 and IL-1β via activation of caspase-1.

Inflammasome is composed of certain member of NLR and procaspase 1 [5, 8, 9] (Figure 1). NLR family members are divided into two groups. One is an NLRP group possessing pyrin domain (PYD), and the other is an NLRC group lacking PYD but possessing caspase recruitment domain (CARD) [19]. NLRP1 (Nalp1), NLRP3 (Nalp3), and NLRC4 (Ipaf) have been demonstrated to nucleate the

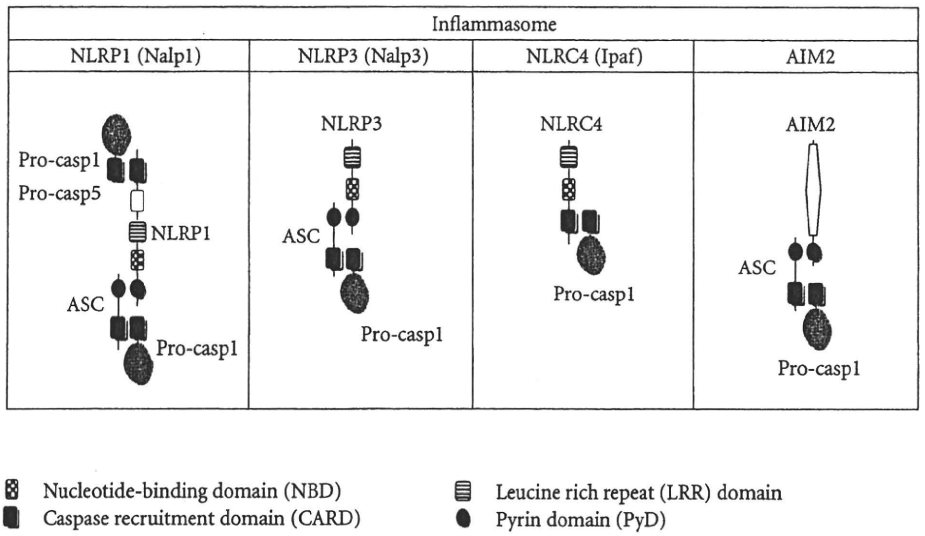

FIGURE 1: Inflammasome constituents. There have been reported at least four types of inflammasomes, NLRP1 (Nalp1), NLRP3 (Nalp3), NLRC4 (Ipaf), and AIM2 inflammasomes. NLR is subdivided into two groups, PYD-possessing group, namely, NLRP and PYD-lacking group NLRC. After exposure of cells to the corresponding stimuli, these NLRs and AIM2 are believed to be self-oligomerized. As it contains CARD at an N-terminus and PYD at a C-terminus, self-oligomerized NLRP1 can recruit procaspase (casp)-1 and procaspase-5 by action of its CARD and also assembly procaspase-1 with help from ASC that possesses both PYD and CARD. Self-oligomerized NLRP3 recruits procaspase-1 by interposing ASC between them. In contrast, self-oligomerized NLRC4 recruits procaspase-1 by directly interacting CARD of procaspase-1 with its CARD. AIM2, belonging a different protein family, is also believed to be self-oligomerized after recognition of double-stranded DNA and recruits procaspase-1 with help from ASC. NLR, Nod-like receptor; CARD, caspase recruitment domain; PYD, pyrin domain.

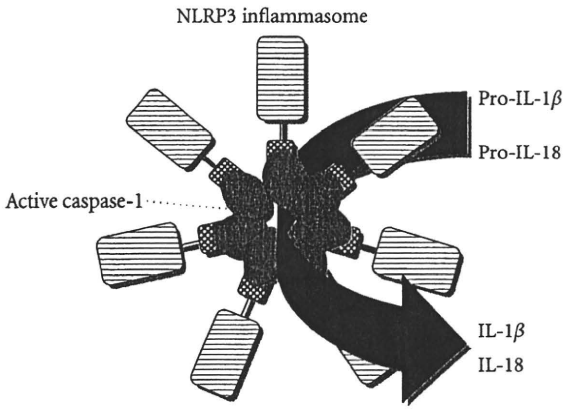

FIGURE 2: A possible schema for IL-18/IL-1β processing by the inflammasome. After appropriate stimulation, the NLRP3 inflammasome is activated to induce active caspase-1, which eventually results in conversion of pro-IL-18/pro-IL-1β into biologically active IL-18/IL-1β.

inflammasomes [5, 19]. In the inflammasome these NLRs are believed to sense cytoplasmic PAMPs exemplified by LPS presumably via their leucine rich repeat (LRR) domain. LRR domain of NLRP3 can recognize all of the TLR agonists except for TLR5 agonist, flagellin of bacterial flagellum, while that of NLRC4 senses flagellin [20]. After being stimulated the NLRs are self-oligomerized by binding each other using their nucleotide-binding domain (NBD). Self-oligomerized NLRP1 directly recruits procaspase-1 by homophilic protein-protein interaction between its N-terminal CARD and CARD of procaspase1 and/or procaspase-5 [8]. ASC consisting of PYD and CARD is regarded as an adapter protein for caspase-1 activation. The NLRP1 can bind to PYD of ASC by its PYD domain at C-terminus, and CARD of ASC eventually recruits procaspase-1 by CARD-CARD interaction (Figure 1). The same scenario can be sketched for the recruitment of procaspase-1 around the oligomerized NLRP3-ASC complexes (Figure 1). NLRC4 has CARD but not PYD. Upon appropriate stimulation of NLRC4, procaspase-1 is recruited onto NLRC4 directly by CARD-CARD interaction (Figure 1). Recently, AIM2, belonging to a different protein family namely PYHIN, was reported to activate caspase-1 by sensing cytoplasmic ds-DNA [7, 21–25]. After recognition of ds-DNA by HIN 200 domain of it, AIM2 might be self-oligomerized for recruitment of procaspase-1 by similarly interposing ASC between these two proteins (Figure 1). Recruitment of procaspase-1 into these inflammasomes is likely to activate caspase-1, leading to conversion from pro-IL-18 and pro-IL-1β into active IL-18 and IL-1β [26] (Figure 2).

As previously reported, mice having received heat-killed *Propionibacterium acnes* are highly susceptible to LPS [27–30]. *P. acnes*-primed mice suffer from liver injuries after LPS challenge. However, administration of neutralizing anti-IL-18 antibodies (Abs) just before LPS challenge can prevent *P. acnes*-primed mice from the liver injury [17]. Besides, *Il18*$^{-/-}$ mice are resistant to the *P. acnes*/LPS treatment [18]. Thus, IL-18 is important for the development of liver injuries.

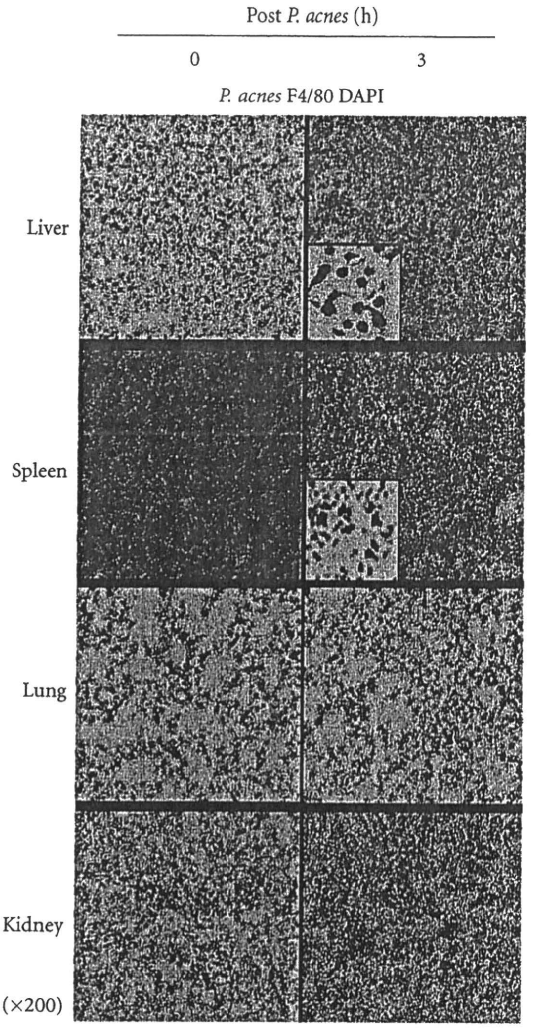

FIGURE 3: Kupffer cells promptly capture heat-killed *P. acnes*. Cy3-labeled, heat-killed *P. acnes* (red) were administered into naïve wild-type mice through a tail vein, and at 3 h tissue specimens were sampled. Frozen tissue slices were incubated with anti-F4/80 mAb (green) and DAPI for detecting macrophages and cell nuclei, respectively. F4/80$^+$ cells (Kupffer cells) capture *P. acnes*, while both F4/80$^+$ and F4/80$^-$ cells ingest them in the spleen. In contrast to live and spleen, both lung and kidney rarely contain *P. acnes*. Magnification of insets is x800.

Here, we review the mechanisms for the *P. acnes*/LPS-induced liver injuries, particularly focusing on those how active IL-18 is released. Prior to addressing this, we would like to introduce the cellular and molecular mechanisms by which pretreatment with *P. acnes* render mice highly susceptible to LPS.

2. Endotoxin Shock Syndrome in *P. acnes*/LPS-Treated Mice

Hypothermia, hypercoagulation (disseminated intravascular coagulation; DIC), high lethality, and tissue injuries are major clinical manifestations of endotoxin shock syndrome [30–35]. After challenge with a subclinical dose of LPS, naïve wild-type (WT) mice do not show these signs (Table 1). In contrast, mice having received heat-killed *P. acnes* 7 days before are highly susceptible to LPS. *P. acnes*-primed mice, but not naïve mice, show obvious and gradual reduction of rectal temperature, serum elevation of proinflammatory cytokines including IL-6, IFN-γ, and TNF-α, high mortality and liver injuries after challenge with the same subclinical dose of LPS [18, 30, 32]. LD_{50} to LPS in *P. acnes*-primed mice is a thousandth or less of that in naïve mice [30]. Furthermore, they exhibit severe hypercoagulation status, which is monitored by plasma levels of coagulation indicator, thrombin antithrombin complexes (TAT), and anti-fibrinolytic protein, plasminogen activator type 1 (PAI-1) that potently inhibits fibrinolysis by blocking conversion from plasminogen into fibrinolytic plasmin [32, 36]. *P. acnes*-primed mice, but not naïve mice, tremendously increase plasma levels of TAT and PAI-1 after LPS challenge [32]. Thus, *P. acnes* treatment powerfully sensitizes mice to LPS.

3. Kupffer Cell Ingestion of Heat-killed *P. acnes*

P. acnes, a Gram-positive bacterium, is often detectable on human skin and has been believed to be relevant to various inflammatory diseases, such as synovitis, acne, pustulosis, hyperostosis, and osteitis (SAPHO) and sarcoidosis [37]. What happens in mice treated with heat-killed *P. acnes*? To address this, we labeled heat-killed *P. acnes* by Cy3, injected them into WT mice through a tail vein, and sampled various tissue specimens at 3 h. We examined tissue distribution of Cy3$^+$ particles by confocal microscopic analyses. Expectedly, heat-killed *P. acnes* are accumulated in the liver and spleen, whereas they were almost absent in the lung and kidney (Figure 3). F4/80$^+$ cells principally capture *P. acnes* in the liver, while both F4/80$^-$ cells and F4/80$^+$ cells ingest them in the spleen (Figure 3).

At day 7 after *P. acnes* treatment tremendous hepatosplenomegaly is observed (Figure 4(a)). The liver doubles its normal weight, whereas weight of spleen achieve more than 5 times (Figure 4(b)). In contrast to the liver and spleen, weight of kidney or lung remains unchanged. In the liver, the dense granulomas primarily consisting of F4/80$^+$ macrophages develop, in the center of which *P. acnes*-ingested F4/80$^+$ Kupffer cells are localized (Figure 4(c)), suggesting that *P. acnes*-ingested F4/80$^+$ Kupffer cells might recruit many F4/80$^+$ macrophages. Immunostaining using rhodamine-conjugated anti-F4/80 mAb followed by counterstaining with hematoxylin reveals that abundant F4/80$^+$ cells are present in the hepatic granulomas [38]. In contrast to the liver, obvious accumulation of F4/80$^+$ cells around *P. acnes* is absent in the spleen (Figure 4(c)). Many dendritic cells were reported to compose the hepatic granulomas as well [39, 40]. *P. acnes* treatment increases hepatic F4/80$^+$ cell number to 30 times and more of that in naïve mice, while the splenic F4/80$^+$ cell number reaches only less than 5 times (Figure 4(d)). Furthermore,

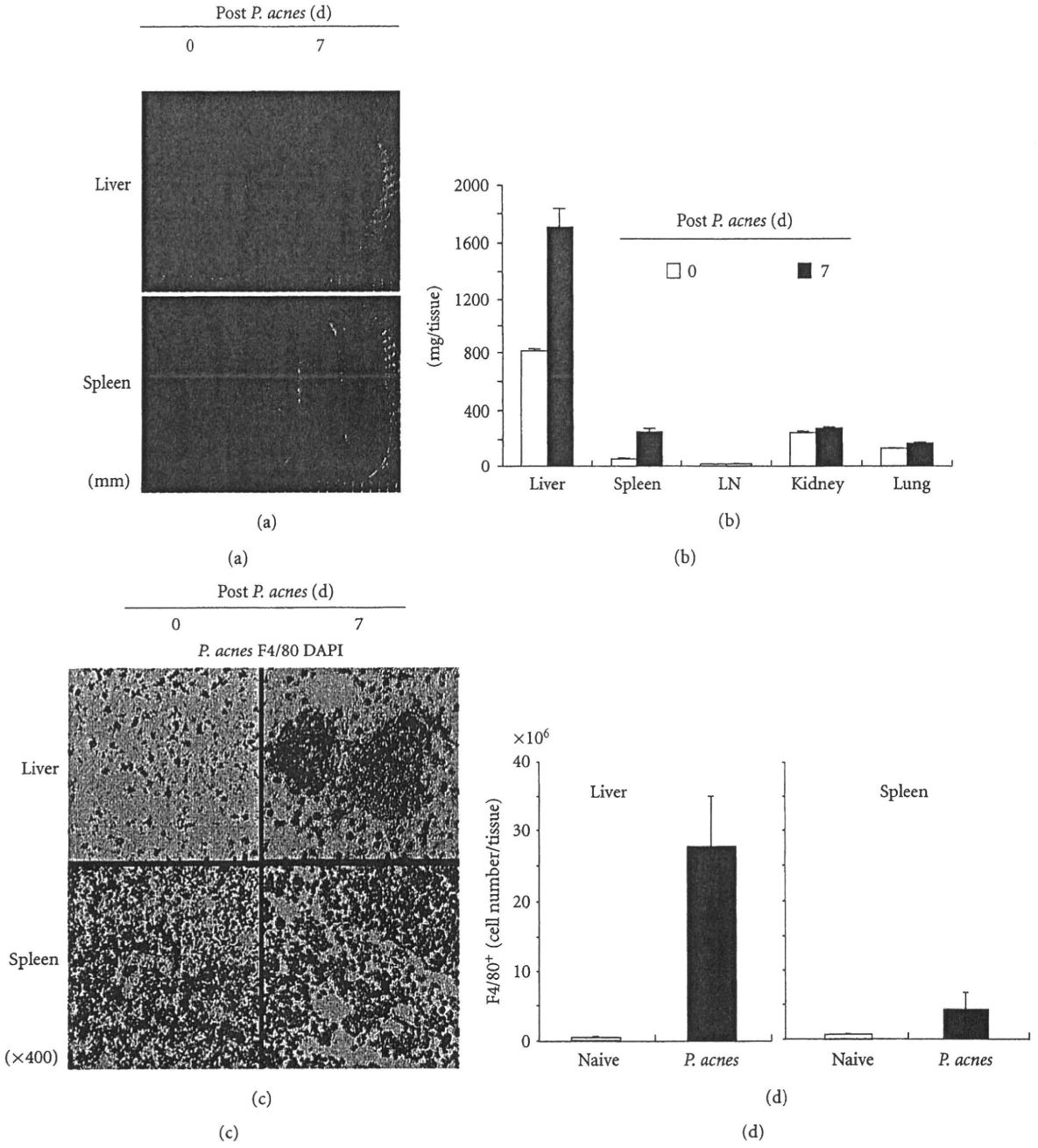

FIGURE 4: Hepatosplenomegaly and hepatic granulomas in *P. acnes*-primed mice. Wild-type mice received Cy3-labeled, heat-killed *P. acnes*, and at day 7 various tissues were removed and weighed (a, b). The liver slices were stained with anti-F4/80 mAb and DAPI for detecting macrophages and cell nuclei, respectively (c). Kupffer cells and splenocytes were prepared from *P. acnes*-primed (closed) or naïve mice (open). After staining with anti-F4/80 mAb, proportion of $F4/80^+$ cells were determined by FACS, and total $F4/80^+$ cell number was counted.

splenic macrophages from *P. acnes*-primed mice produce much higher levels of proinflammatory cytokines including TNF-α in response to LPS than do those from naïve mice [32]. This is also the case for Kupffer cells. Thus, *P. acnes* treatment induces both numerical increase and qualitative alteration of macrophages in the liver and spleen. This may implicate the importance of macrophages for the accomplishment of the LPS sensitization by *P. acnes* treatment.

4. Requirement of Macrophages for the Sensitization to LPS Induced by *P. acnes* Treatment

Depletion of macrophages rescues *P. acnes*-primed mice from the liver injury and high mortality induced by the subsequent challenge with LPS [38] (Table 1). This clearly demonstrates the indispensability of macrophages for the *P. acnes*-induced sensitization to LPS. Intravenous injection of